WOOD AND FIBER SCIENCE

JOURNAL OF THE SOCIETY OF WOOD SCIENCE AND TECHNOLOGY

VOLUME 18 OCTOBER 1986 NUMBER 4

FRACTURE BEHAVIOR OF ADHESIVE JOINTS IN POPLAR

Buhnnum Kyokong,[1] *Frederick J. Keenan,* and *Stephen J. Boyd*[2]

Faculty of Forestry, University of Toronto
Toronto, Ontario M5S 1A1, Canada

(Received August 1984)

ABSTRACT

This study investigated the fracture behavior of poplar-resorcinol gluebonds and determined the respective ranges of applicability of Griffith's brittle fracture theory, Rice's J-integral theory, and Eringen's nonlocal theory. Three-point bending (TPB) specimens of 27 replications for each crack length (0, 3.2, 6.4, and 12.7 mm) for a total of 108 specimens were tested in flexure by the bending normal-to-glueline method. Circular-bar tension (CBT) specimens of 18 replications were tested in tension according to ASTM standard D897-78. Furthermore, compact tension (CT) specimens of 27 replications were tested in cleavage for use as a basis of comparison.

The ultimate bending stress formula corrected for the low span-depth ratio (R_A) was found to be applicable to a TPB specimen with a crack of various lengths. The Griffith brittle fracture, Rice's J-integral, and Eringen's nonlocal theories were all valid in application to poplar-resorcinol joints, provided that the appropriate adjustments are taken into account. On this basis, fracture toughness (K_{IC}) of the joint is approximately 255 kPa$\sqrt{m}$. The percentage of interphase failure was found to correlate well with tensile strength of the gluebonds, but not with cleavage strength.

In addition, microscopic examination of the glue joints revealed that the adhesive flows mainly into the vessels of poplar and that the depth of adhesive penetration depends on gravity. Failure that occurred away from the gluebond in the three-point bending specimens always followed a zone occupied by the largest vessels (weakest link).

Keywords: Cleavage strength, fracture toughness, J-integral, nonlocal theory, wood-adhesive joint, trembling aspen.

INTRODUCTION

Research on improved utilization of fast-growing wood species has increased in many parts of the world in recent years. In Canada, poplar (*Populus* spp.) is one of the fast-growing underutilized hardwoods that currently receives extensive investigation. In addition to other projects on poplar utilization at the University of Toronto, an investigation on the feasibility of using poplar as laminating stock for glued-laminated timber (glulam) is also currently underway (Lepper and Keenan 1985; Wright and Keenan 1985). The present report discusses one phase of

[1] On research leave from Department of Forest Products, Kasetsart University, Bangkok 10900, Thailand.

[2] Presently employed with Morrison Hershfield Ltd., 4 Lansing Sq., North York, Ontario, Canada.

this project, which deals with the assessment of the fracture behavior of side grain bonded trembling aspen, one species of the wood collectively referred to as poplar.

LITERATURE REVIEW

Parameters for assessing quality of wood adhesive bonds

It has been standard practice for a long time to use shear strength and percentage of wood failure from block shear tests (CSA-0112.0) for assessing the quality of wood-adhesive bonds. Using this procedure, Bergin (1964) found that trembling aspen was moderately easy to glue with resorcinol formaldehyde adhesive. Bergin used wood failure percentage as a glueability criterion and pointed out that the initial bond strength was not always a reliable indicator of bonding quality. However, recent research on using natural products (lignin, tannin, etc.) as adhesives revealed that these adhesives tended to develop good strength but low percentages of wood failure (Chow 1983). Other researchers have expressed concern about the effectiveness of the block shear tests in evaluating adhesive-bond quality. Stanger and Blomquist (1965) compared the conventional block shear test to other methods (cross-lap tension and cleavage tests) and concluded that the cleavage test gave the lowest load-carrying capacity and least percentage of wood failure, and consequently had definite advantages over others in evaluating criteria for gluebond quality. Later, Gaudert and Carroll (1974) introduced the bending normal-to-glueline (BN) test, which induced cleavage failure through bending stresses. By comparing this method to the block shear test and the direct tension normal-to-glueline (TN) test, they found that the BN test yielded equivalent results to the TN test and appeared to be more closely related to gluebond quality than was the block shear test. Keenan et al. (1981) have successfully applied the BN test (Fig. 1a) to examine the bonding strength and durability of gluelines in hot-press glulam beams removed from service.

Because of the promising results of the cleavage mode of gluebond failure, the concepts of fracture mechanics have been introduced to evaluate the quality of wood-adhesive joints. White (1977) applied the compact tension (CT) test, Fig. 1b, to evaluate the effect of resin penetration on fracture toughness of wood-adhesive bonds. The sensitivity of the CT test to induced changes of wood and glueline properties (density, surface condition, grain angle, glueline thickness) on bond toughness was further investigated by Ruedy and Johnson (1979) and White and Green (1980). It was concluded that the CT test is applicable to wood-adhesive systems. A few years later, Ebewele et al. (1979) evaluated the applicability of another fracture test method called the tapered double-cantilever beam (TDCB) test, Fig. 1c, to wood-adhesive joints by studying the effects of grain orientation, glueline thickness, and cure time on fracture energy. Follow-up work on the influences of surface aging and surface roughness on fracture energy was also reported (Ebewele et al. 1980). Recently, Dinwoodie (1983) reviewed methods for examining bond quality and durability of wood-adhesive joints and pointed out that the TDCB test, coupled with the theory of fracture mechanics, provides a most effective and sensitive tool for evaluating initial quality and predicting durability of bonded joints.

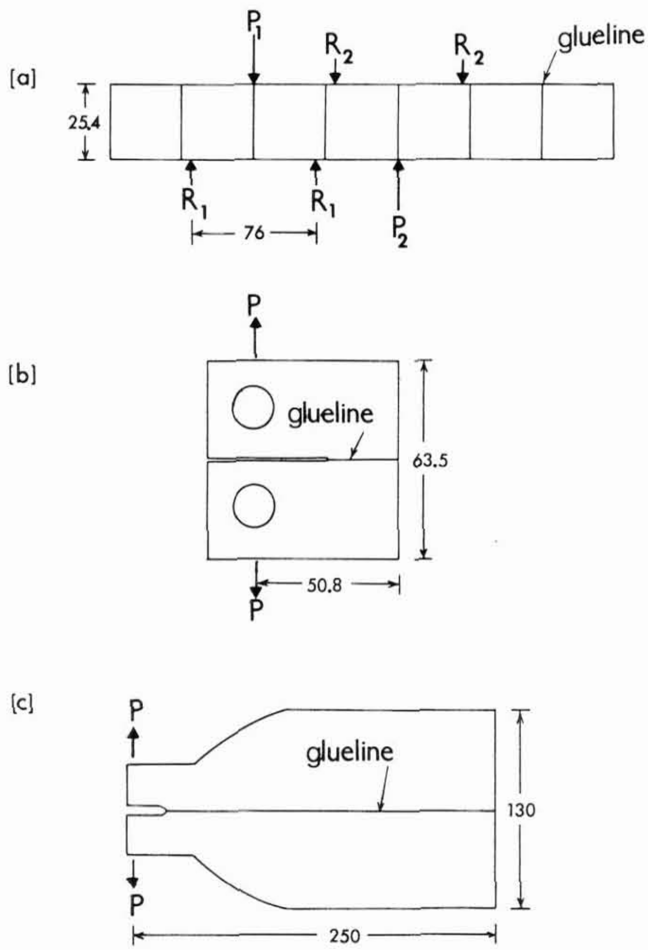

FIG. 1. Specimen geometry and loading condition of test methods that have been applied to wood-adhesive joints (dimensions are in mm): (a) bending normal-to-glueline test (Keenan et al. 1981); (b) compact tension test (White 1977); (c) tapered double-cantilever beam test (Ebewele et al. 1979).

Concepts of fracture mechanics and applications to wood

1. *Classical theory (linear-elastic regime).*—In classical (or local) theory, a material is regarded as a continuous medium of which the state of stress at any point in the body is influenced only by the infinitesimal neighborhood about that point. Mechanical behavior is thus represented by relating stress at a point to strain at a point. Based on this principle and assuming a linearly elastic isotropic material, the concept of linear elastic fracture mechanics (LEFM) was developed (see Liebowitz 1968). It was first presented by Inglis in 1913 in terms of a stress concentration factor (k). For a material having an elliptical crack of length 2c with a minimum radius of curvature r and subjected to applied stress σ_a at a remote distance (Fig. 2a), the concentrated stress at the tip (σ_c) of the crack was given by Inglis as:

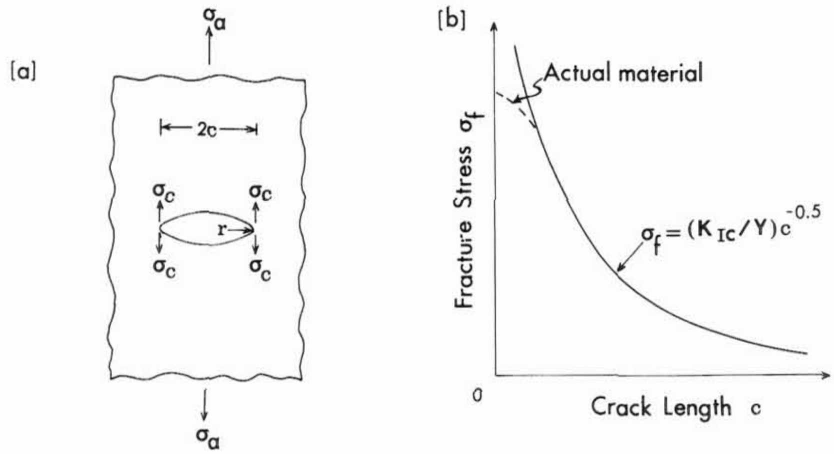

FIG. 2. Griffith's brittle fracture model: (a) an infinite plate containing an elliptical crack of length 2c subjected to applied stress (σ_a) showing stress concentration at the crack tip (σ_c); (b) relation of fracture stress (σ_f) and half crack length (c) based on Griffith theory (K_{IC} = fracture toughness, Y = correction factor).

$$\sigma_c = 2\sigma_a(c/r)^{1/2} = k\sigma_a \tag{1}$$

This equation is obviously not practical when the crack tip is sharp.

Later in 1920, Griffith introduced an alternative energy-balance approach to solve the sharp crack-tip problem. He postulated that the total potential energy (U) of an infinite plate containing a crack (Fig. 2a) equals the summation of the strain energy of an uncracked body ($\sigma_a^2/2E$), the strain energy released due to the introduced crack ($\pi\sigma_a^2c^2/E'$), and the increase in energy according to surface tension of the crack surface ($4\gamma c$):

$$U = \tfrac{1}{2}\sigma_a^2/E - (\pi\sigma_a^2c^2/E') + 4\gamma c \tag{2a}$$

At equilibrium (a critical condition just prior to crack propagation), σ_a approaches fracture stress (σ_f) and $du/dc = 0$. Eq. (2a) becomes the so-called Griffith fracture criterion as:

$$\pi\sigma_f^2c/E' = 2\gamma \tag{2b}$$

where E' equals E for plane stress, and is $E/(1 - \nu^2)$ for plane strain (E = Young's modulus, ν = Poisson's ratio); γ = surface tension energy. Although this expression contains no radius of curvature (r), the assignment of γ for a solid surface is not as practically obvious as in a liquid.

Griffith's theory became practical when Orowan in 1955 and Irwin in 1957 independently introduced the idea in refinement of the concept to include a dissipative energy due to plastic work at the crack tip. Irwin defined fracture behavior of a material in three modes: Mode I (opening or cleavage mode), Mode II (sliding or forward shear mode), and Mode III (tearing or transverse shear mode). By considering the energy balance at the vicinity of the crack tip (instead of for the whole body as employed by Griffith) for the Mode I fracture, Irwin introduced a constant, G, to represent the work flowing from the body into the crack front in order to extend the existing crack (strain energy release rate or crack extension force). At the critical condition, G becomes G_{IC}, which can be expressed as:

$$G_{IC} = 2(\gamma + \gamma_p) \tag{3}$$

The right side of Eq. (3) reflects fracture resistance of a material (γ_p = dissipative energy due to plastic deformation). Consequently, G_{IC} is called "fracture toughness" by Irwin. He pointed out that if the size of the plastic deformation zone at the crack tip is very small compared to the crack length, then γ_p can be ignored. This important point justifies the applicability of the Griffith theory to practical engineering materials and implies the equality of Eqs. (2b) and (3):

$$G_{IC} = \frac{\pi \sigma_f^2 c}{E'} \tag{4}$$

Irwin further simplified this relation by introducing K as a material constant called "stress intensity factor" to relate the asymptotic expression of σ_f and c as:

$$K_{IC} = \sqrt{G_{IC}E'} = \sigma_f\sqrt{\pi c} \tag{5}$$

This equation was then modified for a specimen of finite geometry to take the form:

$$K_{IC} = Y\sigma_f c^{0.5} \tag{6}$$

where Y is a correction factor accounting for specimen geometry and loading condition (including $\sqrt{\pi}$). It should also be kept in mind that Eq. (6) is applicable only to brittle fracture or to a material having a negligible amount of plastic deformation at the crack tip. For the specimen containing a very small crack, however, the level of maximum stress is beyond the elastic limit. The plastic deformation is therefore large enough to invalidate Eq. (6) in the same manner as a short column nullifying the applicability of the Euler buckling formula (Rolfe and Barsom 1977) as shown by a dotted line in Fig. 2b.

Although wood is an anisotropic material, crack propagation in the cleavage mode in wood is always along the grain and can be approximated as being isotropic. The validity of Eq. (6) was verified for green eastern black spruce by Atack et al. (1961) and for dry western redcedar by Johnson (1973). They found the same relationship:

$$K_{IC} = Y\sigma_f c^{0.6} \tag{7}$$

and concluded that the Griffith-Irwin concept is approximately applicable to cleavage fracture in wood. The concept was successfully applied to wood-adhesive systems as mentioned earlier (White 1977; Ebewele et al. 1979; Ruedy and Johnson 1979). Presently, a great deal of literature on this topic has been published mostly concerning solid woods.

2. *Classical theory (elastic-plastic regime).*—There are many practical materials in which fracture behavior does not follow linear elastic theory. A material exhibiting a linear (Hookean) response for stress states within a certain limit and a nonlinear response for those outside was classified as an "elastic-plastic material." Certain elastic materials with a deep crack also behave plastically when the failure

stress is approached. In extending the classical theory to cover this type of material, Rice (1968) introduced a parameter called the "J integral," which is expressed for a plane strain case as (Fig. 3a)

$$J = \int_p \left(W\,dy - T\frac{\partial u}{\partial x}\,ds \right) \tag{8}$$

where W = strain energy per unit volume in the elastic case (or dissipative energy in the plastic deformation case), p = path or contour of the integral (a curve surrounding the crack tip), T = traction on the contour (being cut out along the contour as a free body), u = displacement in the direction of T, and ds = increment of distance (arc length) along the path or contour. Rice also proved that J is a path-independent integral, which means that the J value can be determined from any arbitrary contour. This method is applicable to both linear elastic and elastic-plastic materials. In a linear elastic case, J is identical to G (the strain energy release rate). However, for an elastic-plastic case, J represents the stress intensity at the crack tip, which is analogous to K (the stress intensity factor). Details on the derivation and applications of Eq. (8) can be found in Liebowitz (1968).

By considering the practical application of J, Rice et al. (1973) suggested an alternative and equivalent definition of J as:

$$J = \int_0^\delta \left(-\frac{\partial P}{\partial c} \right)_\delta d\delta, \tag{9}$$

or

$$J = \int_0^P \left(\frac{\partial \delta}{\partial c} \right)_P dP \tag{10}$$

These relate J to the more practical parameter, the area under the load (P) versus load-point-displacement (δ) curve. Eq. (9) simply stated that J is the rate of change of the area under the P vs. δ curve with respect to crack length (c). Based on this relationship, they derived a formula for evaluating J for a specimen with a deep crack subjected to three-point bending (center-point loading) as (Fig. 3b):

$$J = \frac{2}{e}\int_0^{\delta_c} P\,d\delta_c = \frac{2A}{be} \tag{11}$$

where δ_c is the load-point displacement due to only the rotation of the crack surface (θ is caused by the bending moment M in Fig. 3b), e is the remaining ligament (beam depth minus crack length), b is the beam width, and A = area under P vs. δ_c curve. It is essential to note that Eq. (10) was derived by neglecting the elastic deformation due to the uncracked portion of the beam. Therefore, this equation works only in the case of a deep crack. The crack has to be deep enough to weaken the remaining ligament, so that the additional deformation of the uncracked portion is negligible. Advantages and limitations of the J-integral method in comparison with other methods in fracture mechanics are clearly summarized by Paris (1976).

In spite of the wide use of the J integral as the fracture criterion for other

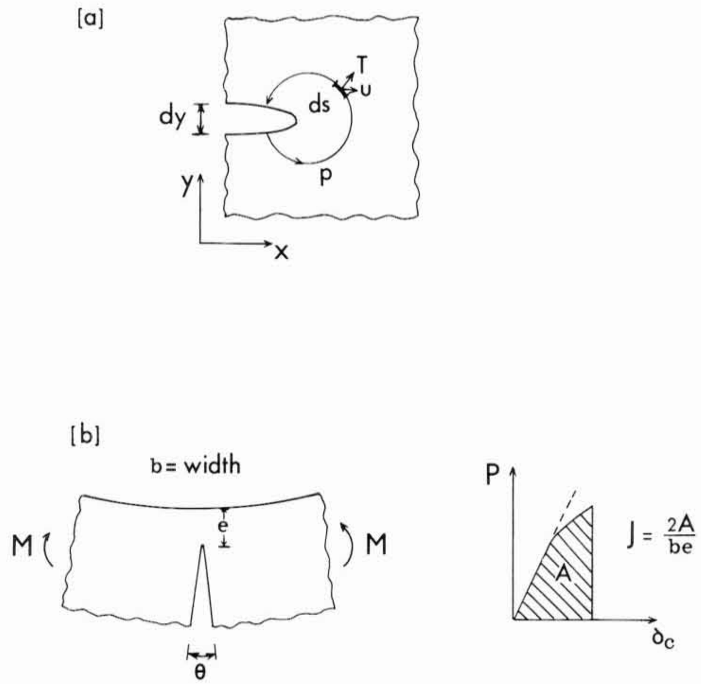

FIG. 3. Rice's J-integral concept: (a) portion of an infinite plate showing path (p) of the J-integral at the crack tip; (b) simplified formula for calculating J-integral of a three-point bending specimen containing a deep crack (M = moment, θ = rotation, b = width, e = remaining ligament, and A = area under the load-deflection curve).

materials, its application to wood products is scarce. Mirza and Mindess (1981) examined the validity of Eq. (8) in application to fracture of a wood beam containing an edge crack perpendicular to grain. They tested a large number of air-dried Douglas-fir beams under third-point loading and found that J could be used as a fracture criterion for wood. Earlier, Komatsu et al. (1976) modified the J integral in Eq. (8) as a fracture criterion for a wood bonded joint. Good applicability of the concept was also found in predicting tensile strength of a double lap joint assembled from air-dried Lawson cypress and rigid epoxy adhesive. Literature on the application of Rice's alternative definition of J, Eq. (11), to wood products has not been found.

3. *Microstructure theory.*—It is commonly agreed that the fracture behavior of a material depends upon its microstructural elements. However, mathematical complexity in formulating a microstructure model slows down the development along this line. So far, attempts have been confined to using a microstructure bonding mechanism to eliminate the unrealistic stress singularity (infinite stress) at the crack tip in the Griffith theory. This approach therefore serves as an extension of the Griffith theory to more closely represent fracture behavior of a material in real life.

For linear-elastic (brittle) materials, Barenblatt proposed in 1962 (see Liebowitz 1968) that there are attraction forces called "cohesive forces" to hold the crack tip together in the cusp form (Fig. 4a) and cancel the stress singularity at the end.

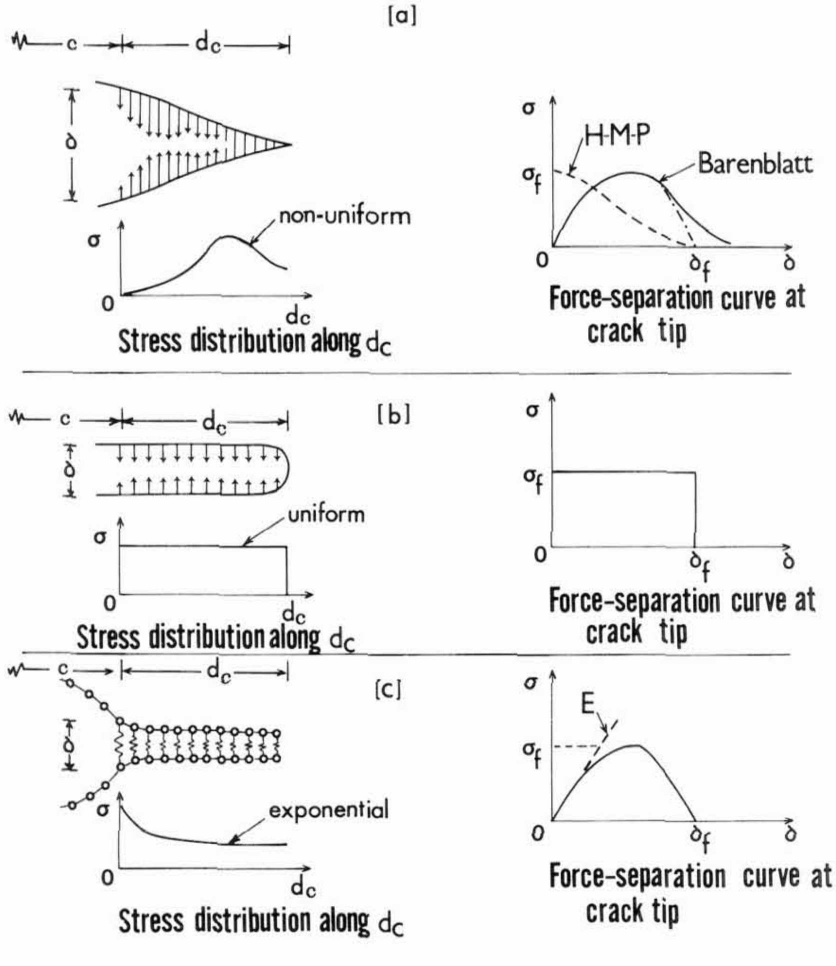

FIG. 4. Fracture models explaining behavior of microstructure at the crack tip (c = half crack length; dc = infinitesimal length of crack extension; σ_f = fracture stress; δ_f = crack-tip separation at failure): (a) Barenblatt model; (b) Dugdale model; (c) Goodier and Kanninen model.

He assumed that the cohesive force distribution along the crack tip is nonuniform, and that the force-separation behavior at the crack tip follows the approximated half sine curve as employed in the "theoretical fracture strength" (see Illston et al. 1979). However, the derivation yielded the same fracture criterion as that of the Griffith theory in Eq. (2). It was also shown by Rice (1968) through the J-integral method that Barenblatt's and Griffith's expressions are equivalent. Later, Hillerborg et al. (1976) modified the J-integral method of representing the Barenblatt theory by assuming the force-separation curve to follow the curve shown as a dotted line (H-M-P) in Fig. 4a. By incorporating their model into the finite element method, a satisfactory verification on tests of unreinforced concrete beams was obtained.

Regarding ductile materials, Dugdale (1960) introduced a fracture concept that was similar to Barenblatt's, except that a uniform tensile yield stress (σ_y) was assumed to hold the plastic yielding zone in front of the crack tip, and that σ_y was assigned to equal the bonding strength between molecules when fracture commenced (Fig. 4b). Assuming finite stress at the crack tip, Dugdale presented the relation between the plastic zone length ratio [dc/(c + dc)] and the applied stress to yield stress ratio (σ_a/σ_y) as:

$$\frac{dc}{(c + dc)} = 2 \sin^2\left(\frac{\pi}{4}\frac{\sigma_a}{\sigma_y}\right) \tag{12}$$

The above concepts are obviously based on a fictitious zone of molecular bonding. A more realistic model was postulated in 1966 by Goodier and Kanninen (see Liebowitz 1968) using nonlinear springs to represent bonds between atom pairs along the crack tip (Fig. 4c). They also adopted the half sine curve to represent the force-separation behavior of the atom pairs, and further assumed the initial slope of the half sine curve to correspond to the elastic constant (E) of the material. By assigning the work done (area under the half sine curve) to the surface energy per unit area (γ), the fracture stress (σ_f) is expressed as (2c = crack length):

$$\sigma_f = \alpha(E\gamma/c)^{1/2} \tag{13}$$

They pointed out that α (a constant) is roughly 1.0 for the above assumption, and is 0.83 if the force-separation curve is assumed to take the exponential form. The 0.83 value of α makes Eq. (13) approximately equivalent to Griffith's expression in Eq. (2b).

Another approach to microstructure theory of brittle fracture is based on the "nonlocal theory" developed by Eringen (1976). As opposed to the local (or classical) theory, this theory states that stress at a point *cannot* be determined entirely by strain at a point, and that the local balance laws are not valid for all parts of the body (they are valid only for the entire body). Nonlocal theory apparently takes the interaction of material sub-bodies into account. Eringen et al. (1977) later applied the theory to abolish the stress singularity in the Griffith fracture criterion. Considering an infinite plate having the same geometry and loading condition as shown in Fig. 2a, they found that the concentrated stress at the crack tip (σ_c) can be computed from:

$$\sigma_c = k(2c/a)^{1/2}\sigma_a \tag{14}$$

where k is a stress concentration factor that relates to the 2c/a ratio as given in Fig. 5 (as before, a = atomic distance). At the critical condition, σ_c equals the cohesive stress between sub-bodies (t_c) and σ_a reaches the fracture stress (σ_f). Substituting Eq. (14) into the Griffith-Irwin expression in Eq. (5) and assigning the convergence value of k = 0.73 to yield:

$$K_{IC} = (\pi/2)^{1/2}\sigma_c\sqrt{a}/k = 1.72t_c\sqrt{a} \tag{15}$$

This equation indicates that t_c becomes infinite as "a" approaches zero. As a consequence, nonlocal theory is the same as local (classical) theory when the significance of material sub-bodies is ignored. The potential of the theory in application to wood products was discussed in detail by Ilcewicz and Wilson (1981). They proposed that Eq. (15) can be made applicable to a material con-

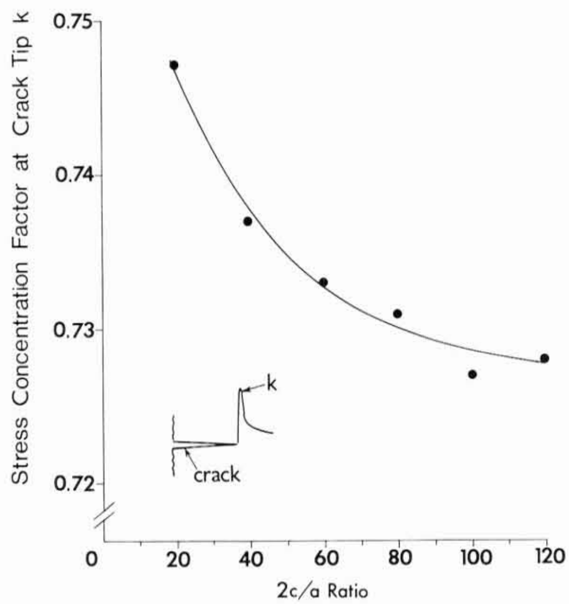

FIG. 5. Relationship of stress concentration factor at the crack tip (k) and 2c/a ratio based on Eringen's nonlocal theory (2c = crack length, a = atomic distance). Note for 2c/a ratio greater than 100; k converges to approximately 0.73. [Plotted from data by Eringen et al. (1977).]

taining no lattice structure such as wood and particleboard by replacing the atomic distance (a) by a characteristic dimension (λ):

$$K_{IC} = (\pi/2)^{1/2}\sigma_c\sqrt{\lambda}/k = 1.72t_c\sqrt{\lambda} \tag{16}$$

The characteristic dimension is defined as the dimension of the critical sub-body that controls fracture behavior. Experimental results satisfactorily verified the validity of Eq. (16) in application to Douglas-fir particleboard.

OBJECTIVES

The objectives of this study were:

1) to determine the validity of Griffith's brittle fracture and Rice's J-integral concept in application to a poplar-adhesive joint using the three-point-bending (TPB) specimen (the same as in a bending normal-to-glueline test);
2) to determine the validity of Eringen's nonlocal theory in application to a poplar-adhesive joint employing the circular-bar tension (CBT) specimen;
3) to evaluate the fracture properties of poplar-adhesive joints using the well-established compact tension (CT) specimen to serve as a basis for comparison (control).

MATERIALS

The lumber was 2- by 4-in. flatsawn trembling aspen (*Populus tremuloides* Michx) obtained from a lumberyard in Southern Ontario in the green condition. It was kiln-dried to a moisture content of 8.5 ± 2%. The adhesive was a resorcinol formaldehyde resin composed of a room-temperature setting liquid adhesive (Cas-

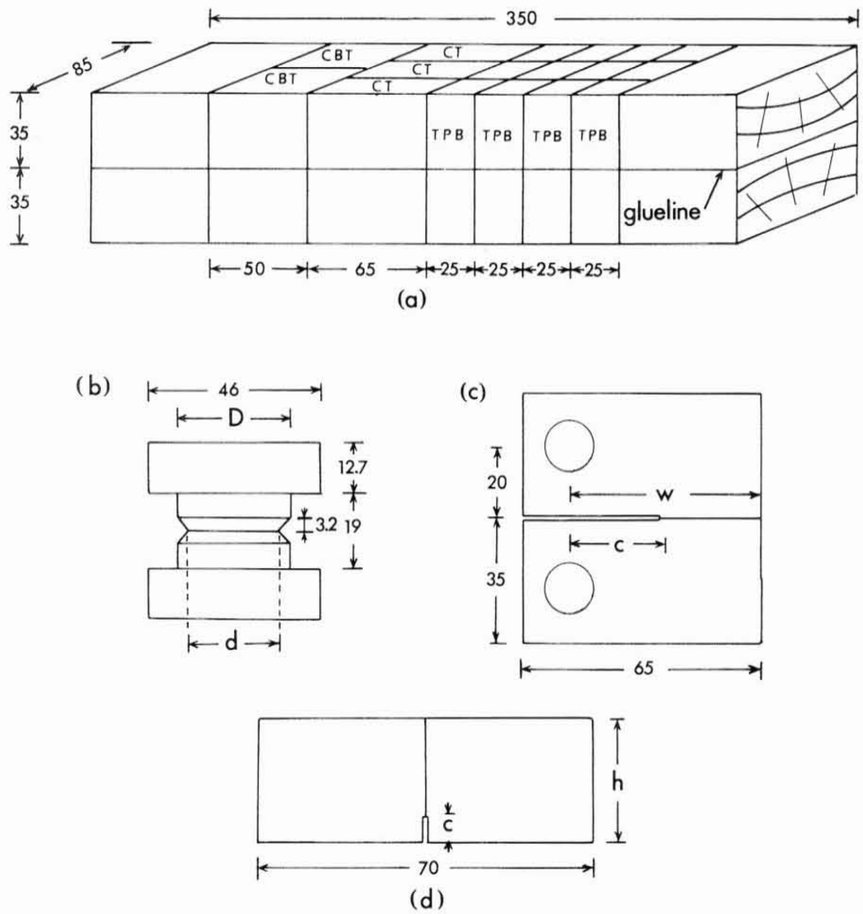

FIG. 6. Preparation of specimens for fracture tests: (a) a poplar-resorcinol joint showing sections for preparation of test specimens (all dimensions are in mm); (b) circular-bar tension (CBT) specimen (D = 27 mm, d = 20 mm); (c) compact tension (CT) specimen (c = 25 mm, w = 50 mm, b = 25 mm); (d) three-point bending (TPB) specimen (h = 25 mm, b = 25 mm, c = 0, 3.2, 6.4, or 12.7 mm).

cophen RS-216) and a powdered catalyst (FM-60M) manufactured by Borden Chemical Co. Adhesive spreading rate was 270 g/m^2 according to an average value recommended by the manufacturer. Other recommendations were that the closed assembly time should not exceed 80 minutes at 21 C and the clamping pressure should be between 0.86 and 1.21 MPa and should be maintained at least 10 hours at 21 C.

EXPERIMENTAL PROCEDURES

The lumber was sawn into billets 38 × 89 × 350 mm in size and classified into three specific gravity classes (0.40, 0.42, and 0.44) of six billets per class. For each class, three replicates of joints were assembled by randomly matching the billet pairs through number drawing. The bonding surface of each billet was planed (with a hand feed jointer) just prior to adhesive application.

The required amount of adhesive was measured with a syringe and spread on

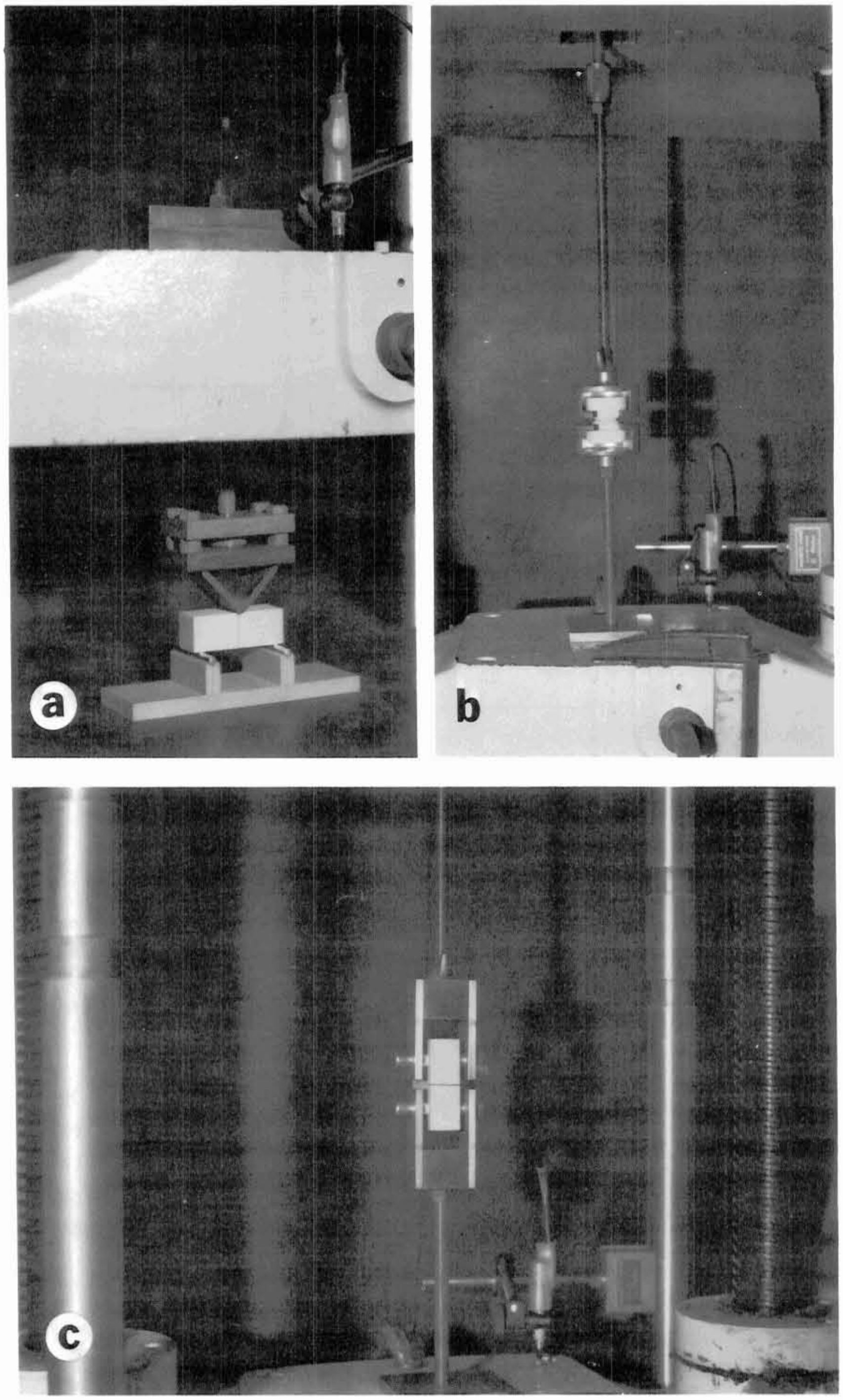

FIG. 7. Set-ups for three-point bending test (a), circular-bar tension test (b), and compact tension test (c).

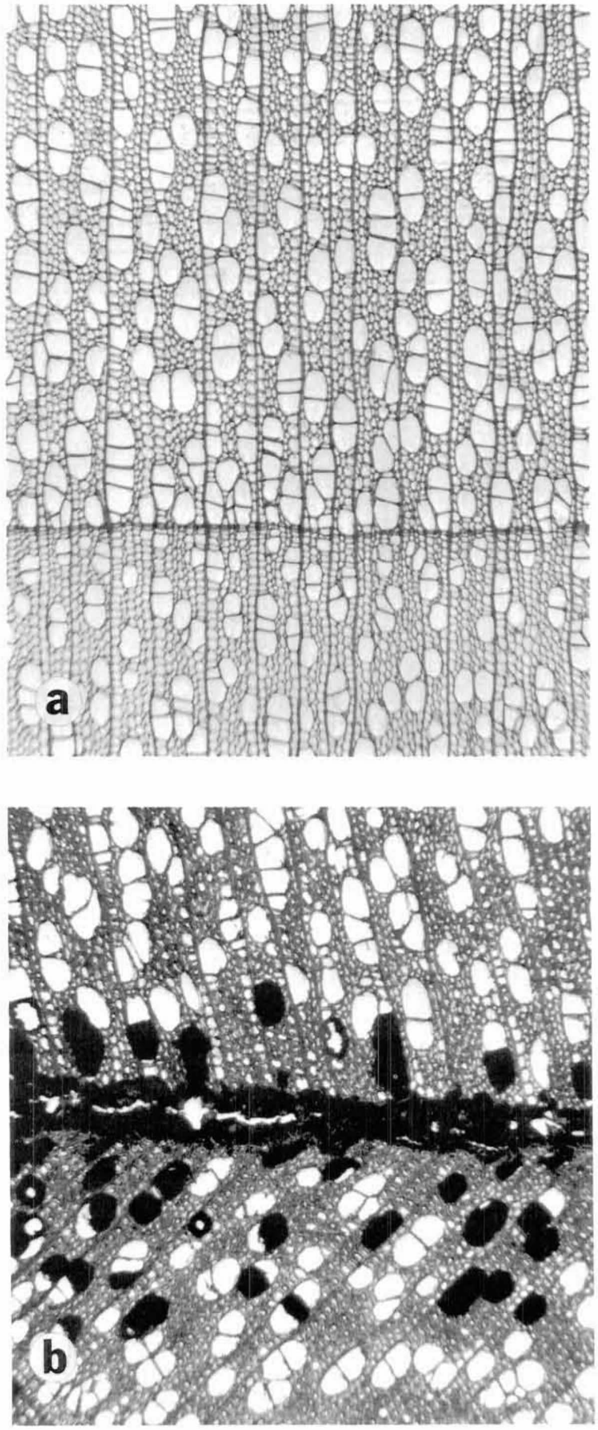

FIG. 8. Microscopic photographs of cross sections of solid trembling aspen showing the weakest zone in earlywood (a), and a poplar-resorcinol joint showing an interphase zone where penetration of adhesive has taken place (b). (The fracture in the glueline was due to the microtoming process.)

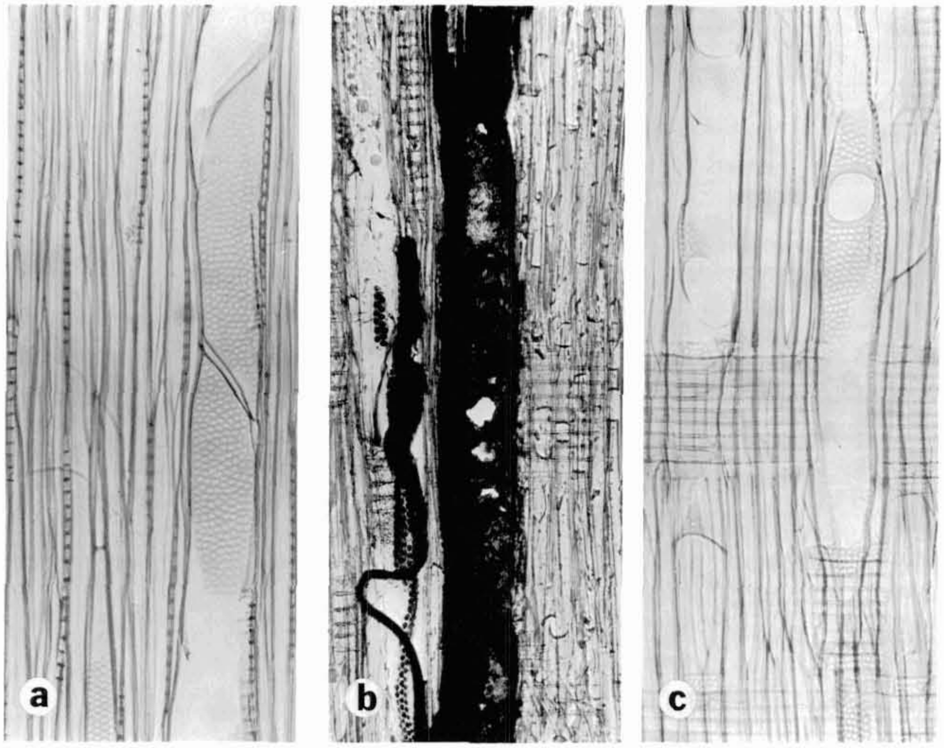

FIG. 9. Microscopic photographs of longitudinal sections of solid trembling aspen in tangential (a) and radial (c) planes, and a poplar-resorcinol joint (b). (Voids in the glueline and buckling of the adhesive in the vessels were caused by the microtoming process.)

both faces of the matching pair of billets using an aluminum plate. The optimal clamping pressure of 0.86 MPa and closed assembly time of 40 minutes determined in a preliminary investigation were employed to bond the assemblies (no significant differences in block shear strength were detected for clamping pressures ranging from 0.86 MPa to 1.21 MPa; however, 40-min closed assembly time produced stronger bonds than either 0 or 80 minutes). The billets were clamped for about 15 hours and subsequently released to be conditioned in a laboratory environment (22 C, 40% RH) for one week, and were subsequently cut into sections for preparation of test specimens as shown in Fig. 6a.

Two circular-bar tension (CBT) specimens were obtained from the first section of the joint by turning in a lathe to the geometry shown in Fig. 6b according to ASTM standard D897-78 (ASTM 1983). The CBT specimen was adopted here because it results in fracture occurring in the interphase zone, defined by White (1977) to be the region where the adhesive penetrates into the wood, and also does not contain any square corners to perturb the tensile stress distribution. In order to determine the fracture behavior of the glue-wood bond, failure should occur in the interphase, which other specimens (such as an internal bond-type) do not assure.

TABLE 1. *Summary of results from three-point bending (TPB) tests of a poplar-resorcinol joint.*

Crack length (mm)	S.G.	Replication	Average R_A (MPa)	Average E_A (MPa)	J_{IC} (N/m)	K_{IC} (kPa$\sqrt{m}$)	Failure percentages Wood	Failure percentages Interphase	Failure percentages Glue	Number of P-δ diagrams I	Number of P-δ diagrams II
0	0.40	9	5.68	190	1,553	533	77	23	0	1	9
	0.42	9	5.25	175	1,312	474	92	8	0	2	7
	0.44	9	7.74	243	2,241	731	58	42	0	2	7
Mean			6.22	203	1,704	580	76	24	0	(5)	(22)
SD			1.37	41	624	144					
Range			4.00–8.84	144–285	795–3,112	361–860					
3.2	0.40	9	2.50	153	382	242	46	54	0	9	0
	0.42	9	2.29	132	392	225	64	36	0	5	4
	0.44	9	3.61	182	599	348	26	74	0	9	0
Mean			2.80	163	458	272	45	55	0	(23)	(4)
SD			0.70	38	132	65					
Range			1.64–4.30	99–239	305–762	175–415					
6.4	0.40	9	1.94	134	314	204	36	64	0	5	4
	0.42	9	1.74	111	326	189	52	48	0	4	5
	0.44	9	2.45	165	402	257	33	67	0	7	2
Mean			2.04	137	348	216	40	60	0	(16)	(11)
SD			0.38	28	81	39					
Range			1.26–2.69	88–190	187–511	141–280					
12.7	0.40	9	1.10	84	256	146	14	86	0	2	7
	0.42	9	1.12	78	310	154	50	50	0	0	9
	0.44	9	1.40	93	379	187	28	72	0	2	7
Mean			1.21	85	315	162	31	69	0	(4)	(23)
SD			0.22	13	84	39					
Range			0.84–1.58	63–115	201–496	118–211					

R_A = adjusted ultimate bending stress, E_A = adjusted modulus of elasticity, J_{IC} = crack extension force (based on J-integral method), K_{IC} = fracture toughness, S.G. = specific gravity based on ovendried weight and volume, SD = standard deviation.

Three compact tension (CT) specimens were machined from the next section with dimensions as shown in Fig. 6c. The remaining four sections were for preparation of three-point bending (TPB) specimens as shown in Fig. 6d. They were sawn into four batches of three TPB specimens; one batch contained no crack (the control; which is identical to the bending normal-to-gluebond test), and the other three contained cracks along the glueline of length 3.2, 6.4, and 12.7 mm, respectively. The crack was first cut with a mini saw (0.5-mm-thick blade) to within approximately 2 mm from the crack tip. A fine crack was then introduced by extending the cut down to the required depth with a razor blade. Care had been taken to align the crack tip within the interphase zone of the joint. All test specimens were stored in a conditioning chamber maintained at 22 C and 50% relative humidity until constant weights were obtained (about two weeks).

The TPB specimens were tested in bending (normal-to-glueline) in the set-up shown in Fig. 7a. The loading head was placed directly on top of the glueline so that the load was applied parallel to the longitudinal grain direction (i.e., the end grain was facing upwards). The loading rate set at 0.1 mm/min for the cracked specimens and 0.2 mm/min for the specimens without cracks in order that fracture would occur within 5 to 10 minutes. The CBT specimens were loaded in tension at 0.4 mm/min as shown in Fig. 7b. The CT specimens were also tested in tension until failure as shown in Fig. 7c. Since the CT tests were for control, the loading rate was set at 5 mm/min according to literature (White 1977; Ruedy and Johnson 1979; White and Green 1980). The rate caused failure to occur in 10 seconds. In the three types of test set-up, possible moment was eliminated using a ball bearing. All tests were performed in a laboratory environment (20 C, 40% RH). Failure loads, load-deformation diagrams, percentage of wood, interphase, and glue failures were recorded. The conventional percentage of wood failure was separated here into wood and interphase failures. Interphase failure is the fracture that occurs within the region where adhesive penetrates into wood. Tears of adhesive and wood therefore appear on both fracture faces. In case of wood failure, only wood grain can be seen on the fracture faces.

In addition, microscopic examinations of the microstructure of trembling aspen, and of the wood-adhesive bonding zone in the vicinity of a typical glueline were also performed. Photographs of the microtomed sections (mounted on slides) across and along the glueline are shown in Figs. 8 and 9, respectively. This information is not only useful in explaining the bonding mechanism, but is also of importance in relating fracture behavior of a wood-adhesive joint to its microstructure.

RESULTS

Three-point bending

The results from the three-point bending (TPB) tests are summarized in Table 1 and correspondingly plotted in Figs. 10 to 13. The adjusted ultimate bending stress (R_A) was determined by the flexure formula corrected to the low span-depth ratio (Timoshenko 1956) as:

$$R_A = \frac{3P_0\ell}{2bh^2}\left(1 - \frac{4h}{3\pi\ell}\right) \tag{17}$$

where ℓ = span, P_o = observed ultimate load (N), and b and h are specimen width and depth in mm, respectively. The correction factor in parentheses was originally derived for a plane stress condition. It is, however, valid for the plane strain condition in this particular loading plane (LR or LT) because of the small Poisson's ratio of wood in this plane (ν_{LR} and ν_{LT} are in the range of 0.009 to 0.07; the second subscript refers to the direction in which the extensional stress occurs; Illston et al. 1979). The difference between plane stress and plane strain has been stated in Eq. (2b).

The adjusted modulus of elasticity (E_A) was computed employing the conventional beam theory formula with the Timoshenko's correction factor as in Eq. (17). The crack extension force (J_{IC}) is therefore equivalent to G_{IC} (the crack extension force based on Griffith's theory), which in turn leads to the calculation of K_{IC} by means of Eq. (5). The recorded load-deformation diagrams fell into two

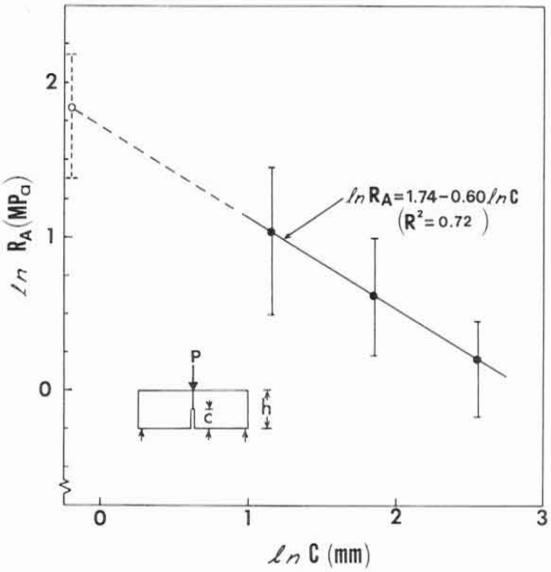

FIG. 10. Plots of adjusted ultimate bending stress (R_A) versus crack length (in natural logarithmic scales) resulting from three-point bending tests. The slope of the regression line is significant at 95% level. (Results from uncracked specimens were excluded from the analysis.)

typical types: linear-elastic behavior (Type I) and elastic-plastic behavior (Type II) as illustrated in Fig. 14.

As shown in Fig. 10, regression of ln R_A on ln c for the three groups of data yields the equation:

$$\ln R_A = 1.74 - 0.60 \ln c \tag{18}$$

This is of the same form as that previously found by others in Eq. (7). It is interesting to note that this relation seems to work for wood, regardless of differences in wood species, moisture content, specimen geometry, and loading conditions. This suggests the possibility of applying Eq. (7) to explain the fracture behavior of wood by taking K_{IR} ($=K_{IC}/Y$) to be the "fracture resistance" for wood. The deviation of Eq. (7) from the Griffith formula (slope = 0.50) is probably caused by an increase in dissipative energy at the crack tip with increasing crack length as indicated by the change in the number of load-deformation diagrams of each type in Table 1. This trend is also evident in the plots by Atack et al. (1961) and by Johnson (1973). On the other hand, the relationship between adjusted modulus of elasticity (E_A) and crack length (c) follows an exponential decay curve as shown by (Fig. 11):

$$\ln E_A = 5.31 - 0.068c \tag{19}$$

Plots of crack extension force (J_{IC}) versus crack length (c) are shown in Fig. 12. J_{IC} represents the amount of energy required to open a unit of crack surface and evidently converges to a constant value (approximately 320 N/m) with deeper crack length. This confirms that J_{IC} is a material constant for a wood-adhesive joint, and that the J-integral method, Eq. (11), is also valid for a wood-adhesive joint, provided that the crack length is deep enough to cause deflection due only

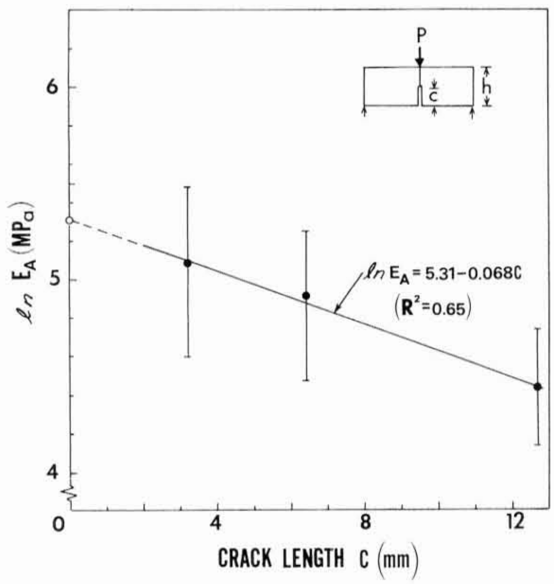

FIG. 11. Plots of adjusted modulus of elasticity (E_A) in natural logarithmic scale versus crack length (c) resulting from three-point bending tests. The slope of the regression line is significant at 95% level. (Results from uncracked specimens were excluded from the analysis.)

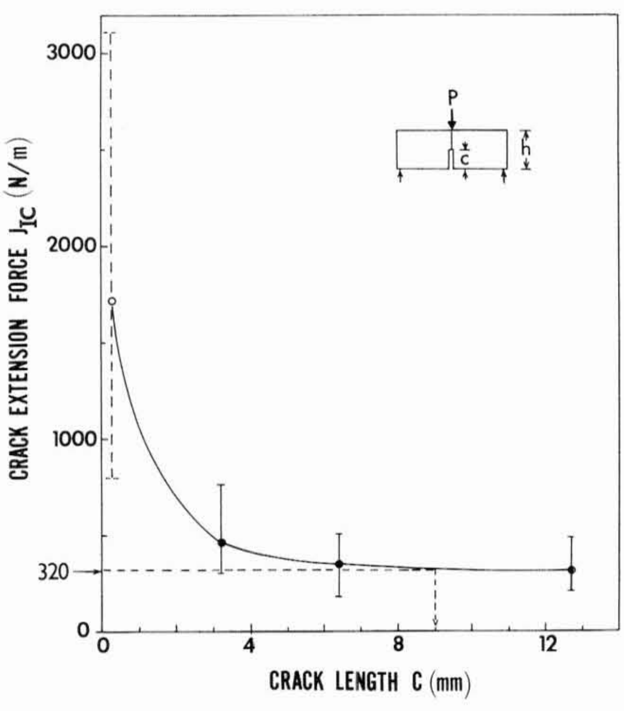

FIG. 12. Plots of crack extension force (J_{IC}) versus crack length (c) resulting from three-point bending tests.

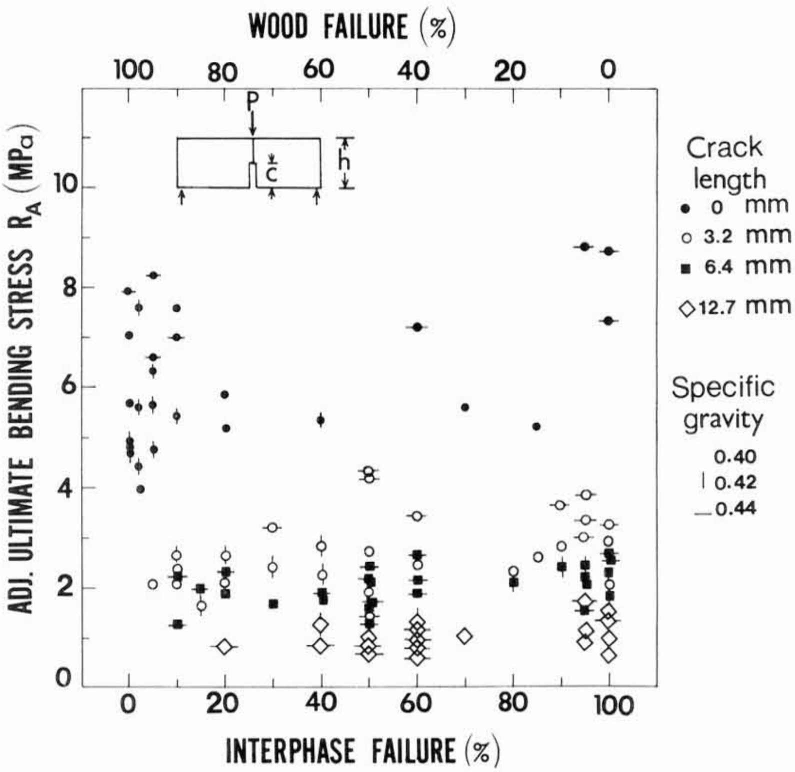

FIG. 13. Scatter diagrams of adjusted ultimate bending stress (R_A) versus percentage of interphase failure at various levels of crack length and specific gravity resulting from the three-point bending test.

to crack opening (no additional deflection induced by strain in other part of the specimen). The required transition crack length (c_t) can be determined as illustrated in Fig. 12 in which, for these test results, c_t is approximately 9 mm. Moreover, the adjusted ultimate bending stresses (R_A) are plotted against the percentages of interphase failure (I) as shown in Fig. 13. The scatter diagram shows no correlation between R_A and I, even within specific gravity and crack length groups. This indicates that the percentage of joint failure in the cleavage mode of fracture does not relate to bonding properties and may not be of practical use in quantifying bond quality.

Circular bar tension

Data from the circular bar tension (CBT) tests are presented in Table 2. The maximum tensile stress (σ_f) was calculated as failure load per unit area of glueline as recommended by ASTM D897-78 (ASTM 1983). No correction for the stress concentration induced at the notch tip had been attempted since a reliable factor was not available. From σ_f, intrinsic flaw size (2c), characteristic dimension (λ), and Eringen's stress concentration factor (k), the fracture toughness (K_{IC}) based on nonlocal theory was computed using Eq. (16). The intrinsic flaw size for wood (3 mm) found by Schniewind and Lyon (1973) was adopted. To obtain the char-

TABLE 2. *Results from circular-bar tension (CBT) tests of a poplar-resorcinol joint.*

S.G.	Joint no.	Specimen no.	Max. tensile stress (MPa) Individual	Max. tensile stress (MPa) Mean (by S.G.)	K_{IC} ($kPa\sqrt{m}$) Local theory	K_{IC} ($kPa\sqrt{m}$) Non-local theory	Failure percentages Wood	Failure percentages Interphase	Failure percentages Glue	P-δ diagram type*
0.40	1	1	3.47		263	240	20	80	0	II
	1	2	2.35		178	162	15	85	0	I
	2	3	3.09		234	213	30	70	0	I
	2	4	2.37		179	164	40	60	0	I
	3	5	2.46	2.65	179	170	50	50	0	II
	3	6	2.15	(SD = 0.51)	161	148	10	90	0	II
0.42	1	7	3.50		260	241	0	100	0	II
	1	8	1.79		123	124	95	5	0	II
	2	9	3.37		254	232	15	85	0	II
	2	10	2.45		185	170	70	30	0	I
	3	11	2.00	2.53	150	138	60	40	0	I
	3	12	2.04	(SD = 0.74)	154	141	80	20	0	I
0.44	1	13	3.04		228	210	10	90	0	I
	1	14	2.28		174	158	60	40	0	I
	2	15	1.97		137	136	95	5	0	I
	2	16	3.11		230	215	50	50	0	I
	3	17	4.03	3.04	297	278	0	100	0	II
	3	18	3.83	(SD = 0.82)	285	265	5	95	0	I
Mean			2.74		204	189	39	61	0	
SD			0.70		53	48				
Range			1.79–4.03		123–297	124–278				

S.G. = Specific gravity based on ovendried weight and volume, K_{IC} = critical stress intensity factor (fracture toughness), * = defined in Fig. 13.

acteristic dimension, examination of the microstructure of the joint in Fig. 8 is necessary to determine the structural level that controls the fracture mechanism. Only the interphase zone is considered here since the main purpose of CBT tests is to induce fracture in this zone. As evident from Fig. 8b, the adhesive flows into vessels and forms rigid rods within the vessels upon curing. The cohesive strength of these rods (resorcinol adhesive) is much higher than that of trembling aspen. When the interphase zone is subjected to tension perpendicular to the grain, it is therefore likely that fracture will occur between the rods. The average diameter of the rods is consequently the structural level that controls fracture in the interphase zone. In other words, the vessel diameter (average) of trembling aspen (100 microns) is the characteristic dimension (λ) for this particular case. Knowing the $2c/\lambda$ ratio, k can be obtained through Fig. 5. The values of K_{IC} can then be computed from Eq. (16). As a basis of comparison, K_{IC} was also calculated using a formula based on local (classical) theory (Hertzberg 1983, p. 281):

$$K_{IC} = PY/D^{3/2} \tag{20}$$

where $Y = 1.72(D/d) - 1.27$, P is load, and D and d are defined in Fig. 6b. Results from these two methods of determining K_{IC} values are plotted in Fig. 15. K_{IC} obtained from nonlocal theory is obviously in good agreement with K_{IC} from local theory. A scatter diagram in Fig. 16 shows a certain degree of correlation ($R^2 = 0.58$) between maximum tensile stress (σ_f) and percentage of interphase (or wood) failure (F_i). Linear regression of σ_f on F_i yields the following equation:

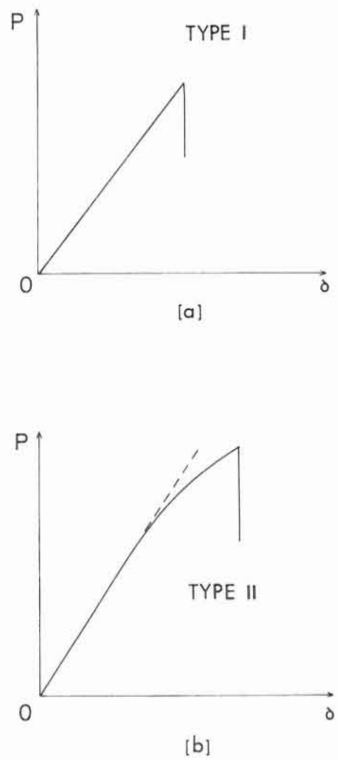

FIG. 14. Two types of typical load-deformation diagrams resulted from three-point bending tests of poplar-resorcinol joints (P = load, δ = deformation): (a) Type I (linear elastic behavior); (b) Type II (elastic-plastic behavior).

$$\sigma_f = 1.73 + 0.016F_i \tag{21}$$

The regression coefficient (slope) of the line is significant at the 95% level.

Compact tension

The results of the compact tension (CT) tests are in Table 3. The load deformation diagram (Fig. 17) indicates that dissipation of energy had taken place before failure, and that a series of crack arrests occurred after propagation. Plots of maximum cleavage load versus percentage of interphase failure in Fig. 18 show no relationship between these two parameters.

Comparison of fracture tests

The values of K_{IC} from the aforementioned tests (TPB, CBT, and CT) are finally compared by plotting in Fig. 19. Evidently, K_{IC} values determined by the J-integral method (TPB tests) at a deeper crack length ($c/h > 0.25$) are in the same order as K_{IC} values based on the nonlocal theory (CBT tests). However, K_{IC} values from the conventional CT tests are higher than the others, which is probably due to the short duration of loading (10 seconds) used in these tests. Also, the calculation of K_{IC} in the CBT test ignored the stress concentration at the notch tip; therefore its true value of K_{IC} is actually larger. Furthermore, the K_{IC} values based on the J-integral method (in Table 1) were calculated employing E_A, which varies with

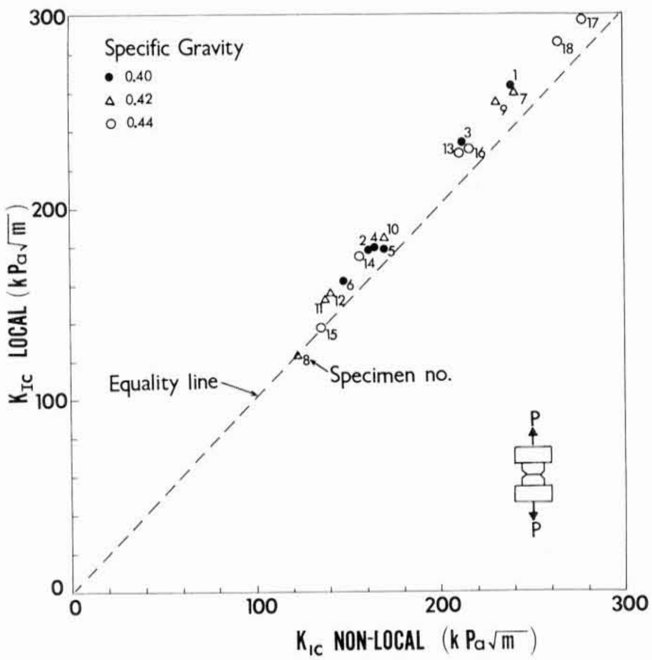

FIG. 15. Plots of fracture toughness (K_{IC}) determined by local theory versus by nonlocal theory resulting from the circular-bar tension test.

crack length (Fig. 11). Since K_{IC} is a material constant, the constant value of J_{IC} from Fig. 12 (320 N/m) and the elastic constant of wood (i.e., mean value of E_A at zero crack length) should be employed in computing K_{IC} from the expression (modification of Eq. (5)):

$$K_{IC} = \sqrt{J_{IC}E_A} \tag{23}$$

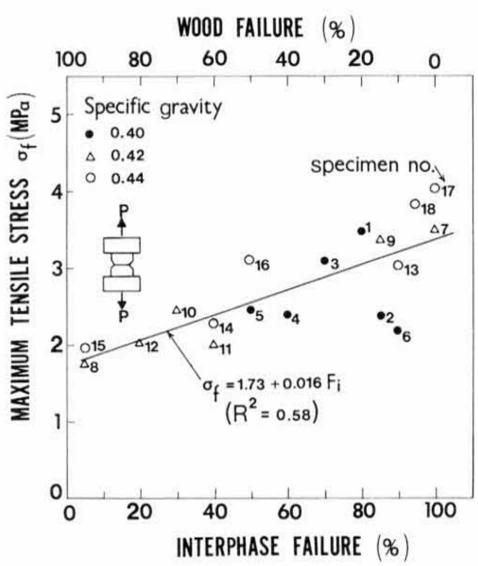

FIG. 16. Scatter diagram of maximum tensile stress (σ_f) versus percentage of interphase failure (F_i) resulting from the circular-bar tension tests.

TABLE 3. *Results from compact tension (CT) tests of a poplar-resorcinol joint.*

S.G.	Joint no.	Specimen no.	Max. load (N)	K_{IC} (kPa$\sqrt{m}$) Individual	Mean (by S.G.)	Failure percentages Wood	Inter-phase	Glue
0.40	1	1	169	290		70	30	0
	1	2	165	287		60	40	0
	1	3	191	319		0	100	0
	2	4	198	320		60	40	0
	2	5	205	336		100	0	0
	2	6	200	331		70	30	0
	3	7	200	327		70	30	0
	3	8	205	335	318	40	60	0
	3	9	187	316	(SD = 18)	90	10	0
0.42	1	10	169	276		50	50	0
	1	11	156	263		95	5	0
	1	12	169	285		100	0	0
	2	13	187	290		95	5	0
	2	14	187	310		95	5	0
	2	15	209	292		60	40	0
	3	16	193	321		100	0	0
	3	17	189	321	298	50	50	0
	3	18	196	323	(SD = 22)	100	0	0
0.44	1	19	247	405		0	100	0
	1	20	271	351		0	100	0
	1	21	222	336		80	20	0
	2	22	298	490		90	10	0
	2	23	222	322		100	0	0
	2	24	245	360		100	0	0
	3	25	242	331		50	50	0
	3	26	222	316	379	95	5	0
	3	27	294	498	(SD = 70)	70	30	0
Mean			209	332		70	30	
SD			37	55		32	32	
Range			156–298	263–498				

S.G. = Specific gravity based on ovendried weight and volume, K_{IC} = critical stress intensity factor (fracture toughness).

The correct value of K_{IC} based on the J-integral concept therefore is 255 kPa$\sqrt{m}$. By considering that the ratio of tensile strength perpendicular to grain for a loading duration of 10 minutes to that of 10 seconds is roughly 0.85 (Barrett and Foshci 1979), the mean value of K_{IC} from the CT tests is adjusted to approximately 255 kPa$\sqrt{m}$. The K_{IC} value from the CBT test would also approach 255 kPa$\sqrt{m}$ if the stress concentration at the notch tip was taken into account.

Effect of adhesive penetration and wood structure

From the microscopic study of the joints, it was found that adhesive penetration into the trembling aspen laminates was affected by gravity as evident in Fig. 8b. More adhesive penetrates into the lower laminate than the upper one. As a result, unequal zones of interphase were formed which might induce an unbalanced stress concentration along the glueline. Bonding strength of an adhesive joint might be improved if this effect could be taken into consideration in the gluing process. In addition, microscopic examination of the failure zone in wood substrate (away from the glueline) of an uncracked TPB specimen indicated that fracture always

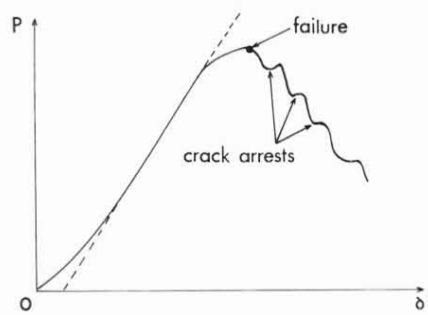

FIG. 17. Typical load (P)–deformation (δ) diagram resulting from compact tension tests. Note the crack arrests occurring after failure.

occurs in the zone of largest vessels (weakest link) not too far from the annual ring (Fig. 8a). This suggests the influence of size and arrangement of vessels in earlywood on cleavage fracture of trembling aspen, which is consistent with the results for other hardwood species obtained by Beery et al. (1983) using stereological techniques.

Bondline thickness effects

It is also interesting to note that the application of the optimal clamping pressure (0.86 MPa) and closed assembly time (40 minutes) to the gluing process produces gluelines of about 90 to 100 microns in thickness, which corresponds to the most optimal glueline-thickness obtained by Ebewele et al. (1979). This confirms the applicability of these parameters for gluing trembling aspen.

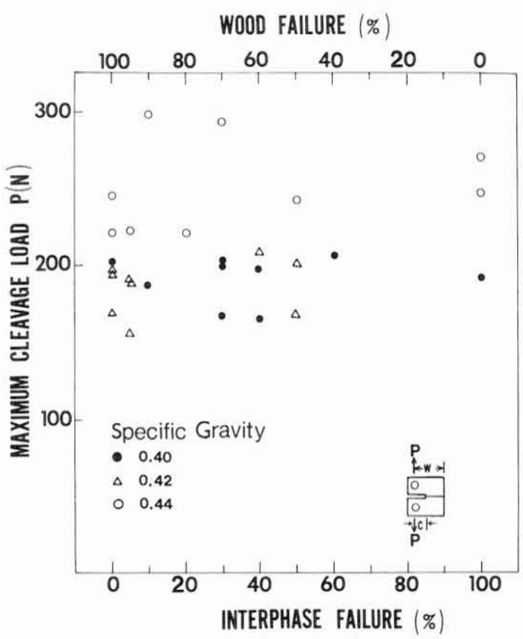

FIG. 18. Scatter diagram of maximum cleavage load versus percentage of interphase failure resulting from the compact tension tests.

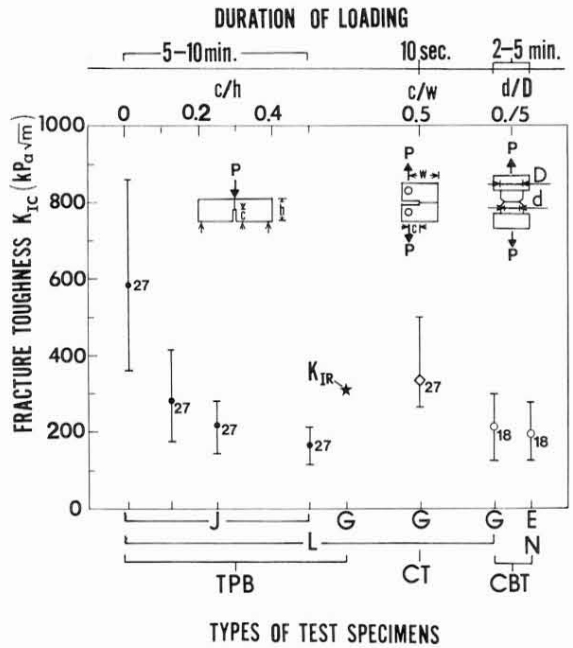

FIG. 19. Comparison of fracture toughness values (K_{IC}) resulting from tests of three-point bending (TPB), compact tension (CT), and circular-bar tension (CBT) specimens. The calculating procedures are based on local theory (L) using the J-integral (J) and the Griffith (G) methods, and on nonlocal theory (N) using the Eringen method (E) (* indicates K_{IR} value calculated by Eq. (b) in the conclusions).

CONCLUSIONS

1. The modified flexure formula for computing ultimate bending stress (R_A) by the bending normal-to-glueline test method:

$$R_A = \frac{3P_0\ell}{2bh^2}\left(1 - \frac{4h}{3\pi\ell}\right) \tag{a}$$

is applicable to poplar-resorcinol joints with or without cracks (symbols defined in Eq. (17)).

2. In determining fracture toughness (K_{IC}) of poplar-resorcinol joints, the modified Griffith's expression in relating R_A to crack length (c) by a new defined fracture resistance for wood ($K_{IR} = K_{IC}/Y$):

$$R_A = K_{IR}c^{-0.6} \tag{b}$$

is valid for brittle fractures (crack not too deep). For a specimen containing a deep crack, K_{IC} can be obtained by means of Rice's J-integral concept of the form:

$$K_{IC} = \sqrt{J_{IC}\,E_A} \tag{c}$$

where $J_{IC} = 2A/be$, A is the area under the load-deformation diagram, b and e are, respectively, the width and the remaining ligament of the specimen; E_A is modulus of elasticity (adjusted for the low span-depth ratio) for a specimen containing no crack. The required depth of a crack (approximately 9 mm) was determined through Fig. 12.

3. The Eringen nonlocal theory for determining K_{IC} based on a circular bar tension (CBT) test is applicable to a poplar-resorcinol joint, provided that the ultimate tensile stress is corrected to account for the stress concentration at the notch tip.
4. The mean value of the fracture toughness of a poplar-resorcinol joint determined by the compact tension (CT) specimen test was 332 kPa$\sqrt{m}$ with loading duration of 10 seconds.
5. When the effects of loading duration, stress concentration, and variable elastic constants are taken into account, all of the above methods yield K_{IC} in the same order of approximately 255 kPa$\sqrt{m}$ for a poplar-resorcinol joint.
6. A relationship between the strength of adhesive bonds and the percentage of interphase failure exists for the circular bar tension test, but does not exist for the three-point bending, nor for the compact tension tests. This finding suggests that the percentage of joint failure in cleavage mode of fracture does not relate to bonding properties, and that the percentage of interphase failure might be of more practical use in quantifying gluebond strength in the tension mode.
7. Microscopic examination of the joints indicated that adhesive flows mainly into vessels (instead of fibers). The depth of adhesive penetration into vessels was also found to be affected by gravity. Moreover, failure of a three-point bending specimen away from the glueline was found to occur in the zone of the largest vessels (weakest link) not too far from the annual ring.

ACKNOWLEDGMENTS

The authors gratefully acknowledge the financial support from the Natural Sciences and Engineering Research Council of Canada (NSERC), and contributions from the following individuals: Serge Dudra, John McCarron, Theo Leonov, and Joe Wright for their help in performing the experiments and obtaining materials; Otto Udvardy of the Borden Chemical Co. for donating the adhesive; Toni Balatinecz and Kay Peng for their assistance with the microscopic work; Lynn Antram, Angie Ciddio, and Hope Coxon for the typing of the manuscript; Professor J. J. Balatinecz and Dr. P. W. T. Peng for their advice and assistance.

REFERENCES

ASTM. 1983. Standard test method for tensile properties of adhesive bonds. ASTM Standard D897-78, American Society for Testing and Materials, Philadelphia, PA.

Atack, D., W. D. May, E. L. Morris, and R. N. Sproule. 1961. The energy of tensile and cleavage fracture of black spruce. TAPPI 44(8):555–567.

Barrett, J. D., and R. O. Foschi. 1979. On the application of brittle fracture theory, fracture mechanics and creep rupture models for the prediction of the reliability of wood structural elements. Pages 1–37 *in* Proceeding of the First Int. Conf. on Wood Fracture. Forintek Canada Corp., Vancouver, BC.

Beery, W. H., G. Ifju, and T. E. McLain. 1983. Quantitative wood anatomy—Relating anatomy to transverse tensile strength. Wood Fiber Sci. 15(4):395–407.

Bergin, E. G. 1964. Gluability and kiln-drying schedules. Can. Wood. Prod. Industries. Pp. 17–19.

CSA. 1977. Definitions and standard test methods for wood adhesives. CSA Standard 0112.0-M1977, Canadian Standards Association, Rexdale, Ontario.

Chow, S. 1983. Adhesive developments in forest products. Wood Sci. Technol. 17(1):1–11.

Dinwoodie, J. M. 1983. Properties and performance of wood adhesives. Pages 1–57 *in* A. Pizzi, ed. Wood adhesives: Chemistry and technology. Marcel Dekker, Inc., New York, NY.

DUGDALE, D. S. 1960. Yielding of steel sheets containing slits. J. Mech. Phys. Solids. 8:100–104.

EBEWELE, R., B. RIVER, AND J. KOUTSKY. 1979. Tapered double cantilever beam fracture tests of phenolic-wood adhesive joints, Part I. Wood Fiber 11(3):197–213.

———, ———, AND ———. 1980. Tapered double cantilever beam fracture tests of phenolic-wood adhesive joints, Part II. Wood Fiber 12(1):40–65.

ERINGEN, A. C. 1976. Continuum physics, Vol. IV. Academic Press, New York, NY. 274 pp.

———, C. G. SPEZIALE, AND B. S. KIM. 1977. Crack-tip problem in non-local elasticity. J. Mech. Phys. Solids 25:339–355.

GAUDERT, P., AND M. N. CARROLL. 1974. The significance of tension normal stresses on the durability of gluelines in laminated timber. Report OPX94E, Eastern For. Prod. Lab., Ottawa, Ontario. 18 pp.

HERTZBERG, R. W. 1983. Deformation and fracture mechanics of engineering materials, 2nd ed. John Wiley & Sons, New York, NY. 697 pp.

HILLERBORG, A., M. MODEER, AND P. E. PATERSSON. 1976. Analysis of crack formation and crack growth in concrete by means of fracture mechanics and finite elements. Cement Concrete Res. 6:773–782.

ILCEWICZ, L. B., AND J. B. WILSON. 1981. Fracture mechanics of particleboard using nonlocal theory. Wood Sci. 14(2):65–72.

ILLSTON, J. M., J. M. DINWOODIE, AND A. A. SMITH. 1977. Concrete, timber, and metals. Van Nostrand Reinhold Co., New York, NY. 663 pp.

JOHNSON, J. A. 1973. Crack initiation in wood plates. Wood Sci. 6(2):151–158.

KEENAN, F. J., J. M. KRYLA, AND M. D. SANDOE. 1981. Strength and durability of hot-press glued-laminated timber beams. Can. J. Civ. Eng. 8(4):509–518.

KOMATSU, K., H. SASAKI, AND T. MAKU. 1976. Application of fracture mechanics to strength analysis of glued lap joints. Wood Res. 61:10–24.

LEPPER, M. M., AND F. J. KEENAN. 1986. Development of poplar glued-laminated timber I: Tensile strength and stiffness of poplar laminating stock. Can. J. Civil Eng. (in press).

LIEBOWITZ, H., ed. 1968. Fracture: An advanced treatise, Vol. II. Academic Press, New York, NY. 759 pp.

MIRZA, F. A., AND S. MINDESS. 1981. Evaluation of J-integral for fracture of wood in tension parallel to grain due to bending. Pages 479–489 *in* A. P. S. Selvadurai, ed. Mechanics of structural media. Elsevier Scientific Publ. Co., Amsterdam.

MULLINS, E. J., AND T. S. MCKNIGHT. 1981. Canadian woods. University of Toronto Press, Toronto, Ontario. 389 pp.

PARIS, P. C. 1976. Fracture mechanics in the elastic-plastic regime. Pages 3–27 *in* Flaw growth and fracture, ASTM STP631. ASTM, Philadelphia, PA.

RICE, J. R. 1968. A path independent integral and approximate analysis of strain concentration by notches and cracks. J. Appl. Mech. 35:379–386.

———, P. C. PARIS, AND J. G. MERKLE. 1973. Some further results of J-integral analysis and estimates. Pages 231–245 *in* Progress in flaw growth and fracture toughness testing, ASTM STP536. ASTM, Philadelphia, PA.

ROLFE, S. T., AND J. M. BARSOM. 1977. Fracture and fatigue control in structures. Prentice-Hall, Inc., Englewood Cliffs, NJ. 562 pp.

RUEDY, T. C., AND J. A. JOHNSON. 1979. Glueline fracture of wood adhesive compact-tension specimens at various grain orientation configurations. Pages 201–218 *in* Proceeding of the First International Conference on Wood Fracture. Forintek Canada Corp., Vancouver, BC.

SCHNIEWIND, A. P., AND D. E. LYON. 1973. A fracture mechanics approach to the tensile strength perpendicular to the grain of dimension lumber. Wood Sci. Technol. 7(1):45–59.

STANGER, A. G., AND R. F. BLOMQUIST. 1965. Block shear, cross-lap tension, and glueline cleavage methods of testing glued joints. Forest Prod. J. 15(12):468–474.

TIMOSHENKO, S. 1956. Strength of materials, Part II. D. Van Nostrand Co., Princeton, NY. 572 pp.

WHITE, M. S. 1977. Influence of resin penetration on the fracture toughness of wood adhesive bonds. Wood Sci. 10(1):6–14.

———, AND D. W. GREEN. 1980. Effect of substrate on the fracture toughness of wood-adhesive bonds. Wood Sci. 12(3):149–153.

WRIGHT, J. M., AND F. J. KEENAN. 1986. Development of poplar glued-laminated timber II: End joints and beams. Can. J. Civil Eng. (in review).